Journal of Organometallic Chemistry 695 (2010) 2068–2075

Contents lists available at ScienceDirect

Journal of Organometallic Chemistry

journal homepage: www.elsevier.com/locate/jorganchem

Osmium assisted C–H activation and C=N cleavage of N-(2′-hydroxyphenyl) benzaldimines. Synthesis, structure and electrochemical properties of some organoosmium complexes

Sumon Nag [a], Judith A.K. Howard [b], Hazel A. Sparkes [b], Samaresh Bhattacharya [a,*]

[a] Department of Chemistry, Inorganic Chemistry Section, Jadavpur University, Kolkata 700 032, India
[b] Department of Chemistry, University of Durham, South Road, Science Site, Durham, DHI 3LE, UK

ARTICLE INFO

Article history:
Received 27 March 2010
Received in revised form
11 May 2010
Accepted 13 May 2010
Available online 20 May 2010

Keywords:
Osmium
N-(2′-Hydroxyphenyl)benzaldimines
C–H activation
C=N cleavage
Decarbonylation

ABSTRACT

Reaction of N-(2′-hydroxyphenyl)-4-R-benzaldimines (**L-R**, R = OCH_3, CH_3, H, Cl and NO_2) with [Os(PPh_3)$_3$$Br_2$] in refluxing 2-methoxyethanol in the presence of triethylamine affords two families of organoosmium complexes (**1-R** and **2-R**). In both **1-R** and **2-R** complexes a benzaldimine ligand is coordinated to the metal center as tridentate C,N,O-donor. In the **1-R** complexes, a bidentate N,O-donor imionsemiquinonate ligand, derived from the hydrolysis of another benzaldimine, and a PPh_3 ligand are also coordinated to osmium. In the **2-R** complexes, a carbonyl, derived from decarbonylation of 4-R-benzaldehyde (derived from the same hydrolysis stated above), and two PPh_3 ligands take up the remaining coordination sites on osmium. Structures of the **1-Cl** and **2-OCH_3** complexes have been determined by X-ray crystallography. All the **1-R** and **2-R** complexes are diamagnetic, and show characteristic ^{1}H NMR signals and intense MLCT transitions in the visible region. Cyclic voltammetry on the **1-R** complexes shows a reversible Os(III)–Os(IV) oxidation within 0.47–0.67 V (vs SCE), followed by an irreversible oxidation of the imionsemiquinonate ligand within 1.10–1.36 V. An irreversible Os(III)–Os(II) reduction is also displayed by the **1-R** complexes within −1.02 to −1.14 V. Cyclic voltammetry on the **2-R** complexes shows a reversible Os(II)–Os(III) oxidation within 0.29–0.51 V, followed by a quasi-reversible oxidation within 1.04–1.29 V, and an irreversible reduction of the coordinated benzaldimine ligand within −1.16 to −1.31 V.

1. Introduction

Utilization of transition metals in promoting useful chemical transformations of organic substrates has been of considerable current interest [1–16]. Such transformations usually proceed via a C–H activation of the organic substrate [17–35], leading to the formation of a reactive organometallic intermediate, which then undergoes further reactions to yield the final product. Transition metal mediated C–H activation of organic molecules is therefore of significant importance and the present work has originated from our interest in this area [36–57]. For the present study, a group of five Schiff base ligands, *viz*. N-(2′-hydroxyphenyl)benzaldimines (**L-R**), derived from *para*-substituted benzaldehydes and 2-aminophenol, have been selected as the target molecules for C–H activation and osmium has been selected as the transition metal for promoting the C–H activation.

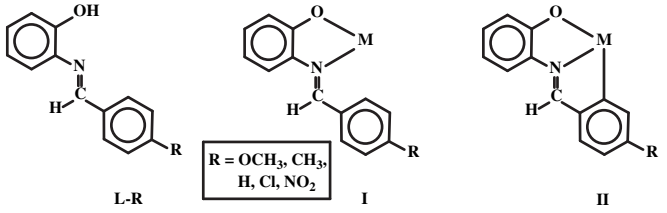

These ligands have two potential donor sites, the phenolate-oxygen and the imine-nitrogen, and hence are expected to bind to metal ions, via dissociation of the phenolic proton, as bidentate N, O-donors forming five-membered chelate ring (**I**). In view of the closeness of the pendent phenyl ring to the metal center in **I**, C–H activation at one ortho position of the phenyl ring leading to the formation of a cyclometallated species (**II**) appears to be a possibility [40,45,58–60]. With the intention of inducing the said C–H activation of the N-(2′-hydroxyphenyl)benzaldimines (**L-R**), their reaction has been carried out with [Os(PPh_3)$_3$$Br_2$]. This particular

* Corresponding author.
E-mail address: samaresh_b@hotmail.com (S. Bhattacharya).

0022-328X/$ – see front matter © 2010 Elsevier B.V. All rights reserved.
doi:10.1016/j.jorganchem.2010.05.015

complex has been picked up as the osmium starting material for this reaction because of its demonstrated ability to promote C–H activation, as well as to accommodate tridentate ligands [51,54]. Reaction of the chosen benzaldimines (**L-R**) with $[Os(PPh_3)_3Br_2]$ has indeed afforded two families of interesting organoosmium complexes, in both of which a benzaldimine ligand is coordinated to the metal center in the expected tridentate C,N,O-fashion (**II**). In addition, a second benzaldimine has undergone some unexpected hydrolytic cleavage of the C=N bond and thus has provided ancillary ligands to complexes of both the types. The present report deals with the chemistry of these organosmium complexes, with special reference to their formation, structure and, spectral and electrochemical properties.

2. Results and discussion

2.1. Synthesis and characterization

Five N-(2′-hydroxyphenyl)benzaldimines (**L-R**) with different *para*-substituents (R = OCH_3, CH_3, H, Cl, and NO_2) in the benzaldimine fragment have been used in the present work in order to study their influence, if any, on the redox properties of the resulting osmium complexes. Reaction of the selected benzaldimines (**L-R**) with $[Os(PPh_3)_3Br_2]$ proceed smoothly in refluxing 2-methoxyethanol in the presence of triethylamine. From each of these reactions two complexes with distinctly different colors were obtained, *viz*. a brown complex of the type **1-R** and a blue complex of the type **2-R** (see Chart 1). The combined yield of these two complexes has been reasonable. Preliminary characterizations (microanalysis, ^1H NMR, IR) on the **1-R** complexes indicated presence of a triphenylphosphine, a benzaldimine ligand, and a third ligand containing one phenyl ring in each of them. In order to find out identity of the third ligand, coordination mode of the benzaldimine, and stereochemistry of the **1-R** complexes, structure of a representative member of this family, *viz*. **1-Cl**, has been determined by X-ray crystallography. The structure is shown in Fig. 1 and selected bond parameters are listed in Table 1. The structure shows that an N-(2′-hydroxyphenyl)-4-chlorobenzaldimine is coordinated to osmium in the targeted tridentate C,N,O-fashion (**II**), via loss of the phenolic proton and activation of an ortho C–H bond in the benzaldehyde fragment. It may be relevant to mention here that example of such osmium-assisted C–H activation is scarce [51,54,61–63]. It may also be noted here that, though relatively less common, this particular

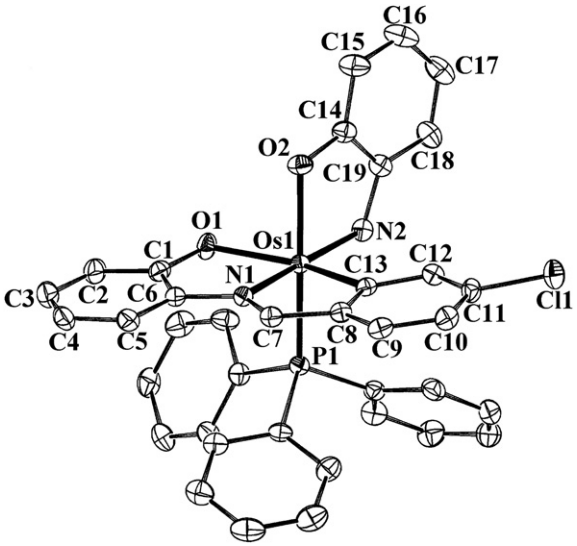

Fig. 1. View of the **1-Cl** complex.

Table 1
Selected bond lengths (Å) and bond angles (°) for **1-Cl** and **2-OCH_3**.

1-Cl		**2-OCH_3**	
Bond lengths (Å)			
Os1–C13	2.054(3)	Os1–C13	2.042(3)
Os1–N1	2.105(2)	Os1–N1	2.083(2)
Os1–O1	2.052(2)	Os1–O1	2.1909(18)
Os1–N2	1.907(2)	Os1–C51	1.842(3)
Os1–O2	2.107(2)	Os1–P1	2.3578(7)
Os1–P1	2.2875(7)	Os1–P2	2.3593(7)
C1–O1	1.333(3)	C1–O1	1.332(4)
C6–N1	1.418(4)	C6–N1	1.409(4)
C7–N1	1.299(4)	C7–N1	1.315(4)
C14–O2	1.319(3)	C51–O3	1.166(4)
C14–C19	1.408(4)		
C19–N2	1.383(4)		
Bond angles (°)			
C13–Os1–O1	151.36(10)	C13–Os1–O1	154.19(11)
P1–Os1–O2	170.62(6)	P1–Os1–P2	171.10(3)
N1–Os1–N2	169.68(9)	C51–Os1–N1	175.55(12)
O1–Os1–N1	76.39(8)	O1–Os1–N1	75.95(9)
N1–Os1–C13	75.65(10)	N1–Os1–C13	78.25(11)
N2–Os1–O2	79.12(9)	Os1–C51–O3	176.9(3)

coordination mode (**II**) of the N-(2′-hydroxyphenyl)benzaldimines has precedence in the literature [40,45,58–60]. An iminophenolate fragment, which appears to have originated from cleavage of another benzaldimine ligand across the C=N bond, is also coordinated to the metal center as a bidentate N,O-donor forming a five-membered chelate ring. Such transition metal mediated C=N cleavage reactions are of significant contemporary interest [64–66]. A triphenylphosphine has satisfied the sixth coordination site on osmium. Within the iminophenolate fragment, the C–O and C–N distances lie between those expected for localized single and double bonds, which clearly indicate that this ligand is coordinated in the iminosemiquinonate form (see **1-R** in Chart 1). It may be noted here that the observed bond distances within the osmium-bound iminophenolate fragment agree well with a similar fragment observed by us before [54]. The Os–P distance, as well as the Os–C, Os–N and Os–O distances, in the remaining part of the complex molecule are all quite normal [51,67–73]. The CN_2O_2POs core is distorted significantly from ideal octahedral geometry, which is reflected in all the bond parameters around osmium. The absence of any solvent of crystallization in the crystal lattice of **1-Cl** indicates possible existence of non-covalent interaction(s) between the individual complex molecules. A closer look at the packing pattern in the crystal reveals that weak inter-molecular interactions of two types, *viz*. C–H···O hydrogen-bonding and π–π stacking, are active in the lattice. A selected view of these interactions is shown in Fig. 2. The π-clouds over phenyl rings of the benzaldimine ligand of two adjacent complex molecules establish a π–π interactions that holds the two molecules together making a dimeric unit. There also exist a pair of C–H···O interactions between the two molecules in the dimeric unit. These dimeric units are linked by another set of C–H···O interactions (Fig. 2). These C–H···O and π–π interactions are extended throughout the entire lattice of **1-Cl**, and seem to assist with the stabilization of the crystal lattice. It may be relevant to note here that such interactions are of significant importance in molecular recognition processes as well as in crystal engineering [74–86]. As all the **1-R** complexes have been synthesized similarly and they show similar properties (*vide infra*), the other four **1-R** (R ≠ Cl) complexes are assumed to have similar structure as the **1-Cl** complex.

Preliminary characterizations on the **2-R** complexes indicated presence of two triphenylphosphines, a benzaldimine ligand, and a carbonyl in each of them. In order to authenticate the composition of these complexes and ascertain coordination mode of the

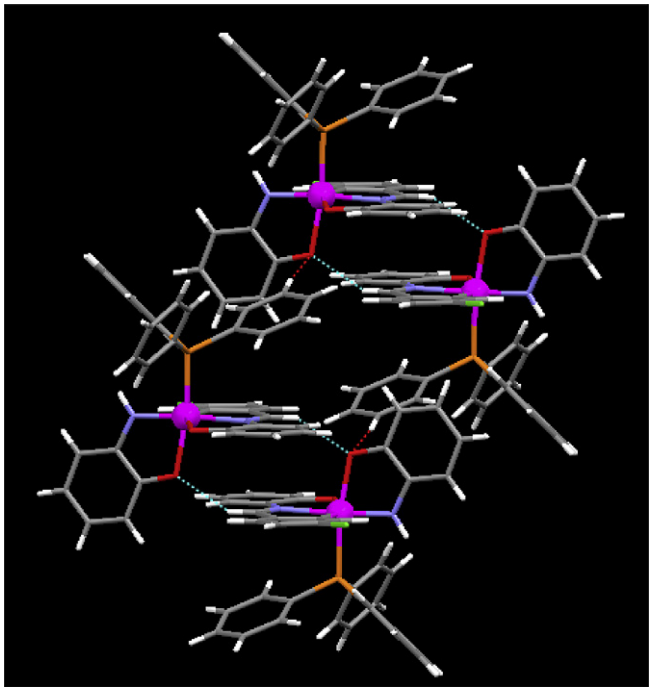

Fig. 2. Hydrogen-bonding and π–π interactions in the crystal lattice of the **1-Cl** complex.

benzaldimine as well as stereochemistry of these complexes, structure of a selected member of this family, *viz*. **2-OCH$_3$**, has been determined by X-ray crystallography. The structure (Fig. 3) shows that, as observed in the **1-Cl** complex, the N-(2′-hydroxyphenyl)-4-methoxybenzaldimine is coordinated to osmium in the similar C,N, O-fashion (**II**). Two triphenylphosphines and a carbonyl are also coordinated to the metal center. Osmium is therefore sitting in a C_2NOP_2 coordination environment, which is distorted octahedral in nature, apparent from the bond parameters around the metal center. The coordinated benzaldimine ligand and the carbonyl have constituted one equatorial plane with the metal at the center, while the PPh_3 ligands have occupied the remaining two axial positions and hence they are mutually *trans*. While most of the bond distances in the Os–CNO chelate are similar to those observed in the **1-Cl** complex (Table 1), the Os–O distance is significantly longer, and the difference may be due to the difference in oxidation state of the metal center as well as difference in the coordination environment around osmium. In the Os–CO fragment, the Os–C and C–O distances are quite normal, and the Os–C–O angle deviates slightly from linearity [87–89]. The Os–P distances are also quite usual, as observed in structurally characterized osmium(II) complexes having a trans $Os(PPh_3)_2$ fragment.[51,54] In the crystal lattice of the **2-OCH$_3$** complex, there exists fraction (75%) of a water molecule per pair of complex molecules, and it is found to be linked with the complex molecule through O–H···O(phenolate) and O···H–C interactions (Fig. 4). The carbonyl oxygen of one complex molecule is hydrogen-bonded simultaneously to phenyl C–H and azomethine C–H of an adjacent complex molecule.

Based on the similarity in synthetic procedure and properties (*vide infra*) of the **2-R** complexes, the other four **2-R** (R ≠ OCH_3) complexes are assumed to have similar structure as the **2-OCH$_3$** complex.

The exact mechanism behind formation of both **1-R** and **2-R** complexes from the same synthetic reaction is not completely clear to us. However, the speculated sequences shown in Scheme 1 seem probable. In the initial step the benzaldimine ligand binds, via loss of the phenolic proton as well as another proton from one *ortho* position of the phenyl ring in the benzaldehyde fragment, to the metal center in $[Os(PPh_3)_3Br_2]$ as a dianinonic tridentate C,N, O-donor. This chelation is also associated with loss of an electron from the metal center and dissociation of one triphenylphosphine to afford a osmium(III) complex as a reactive intermediate (**A**). In the following step **A** undergoes reaction with a second molecule of the benzaldimine ligand generating another intermediate **B**, in which the second benzaldimine binds itself to osmium as a mono-anionic bidentate N,O-donor by displacing the bromide and the triphenylphosphine. The imine function of this N,O-chelated benzaldimine then undergoes hydrolysis generating an amino-phenolate fragment, which remains coordinated to osmium(III) (**C**), and the corresponding free *para*-substituted benzaldehyde. Facile hydrolysis of metal-bound imine function is documented in the literature [64–66]. The coordinated aminophenolate fragment in **C** is believed to undergo further one-electron and one-proton loss [90,91], and thus affords complex **1-R**. The free *para*-substituted benzaldehyde reacts with intermediate **A**, whereby the metal center undergoes a one-electron reduction and the benzaldehyde undergoes decarbonylation, leading to the formation of the carbonyl complex of osmium(II) (**2-R**). To check that the source of carbonyl in **2-R** complexes is the benzaldehyde generated *in situ* and not the solvent 2-methoxyethanol in which the synthetic reactions were carried out, reactions of the N-(2′-hydroxyphenyl)-4-R-benzaldimines (**L-R**) with $[Os(PPh_3)_3Br_2]$ were also carried out in a solvent that cannot be the source of carbonyl, *viz*. benzene, and

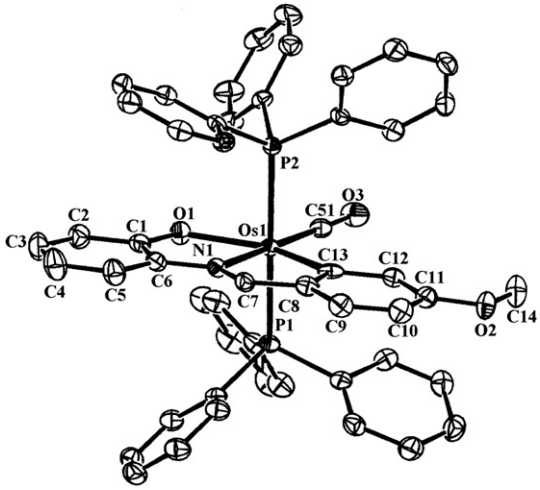

Fig. 3. View of the **2-OCH$_3$** complex.

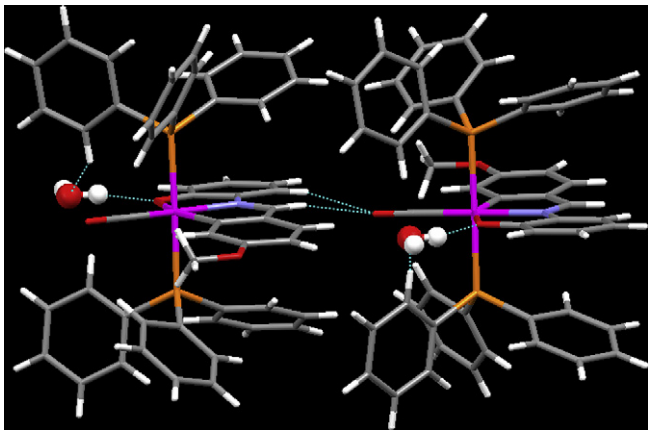

Fig. 4. Hydrogen-bonding interactions in the crystal lattice of **2-OCH$_3$** complex.

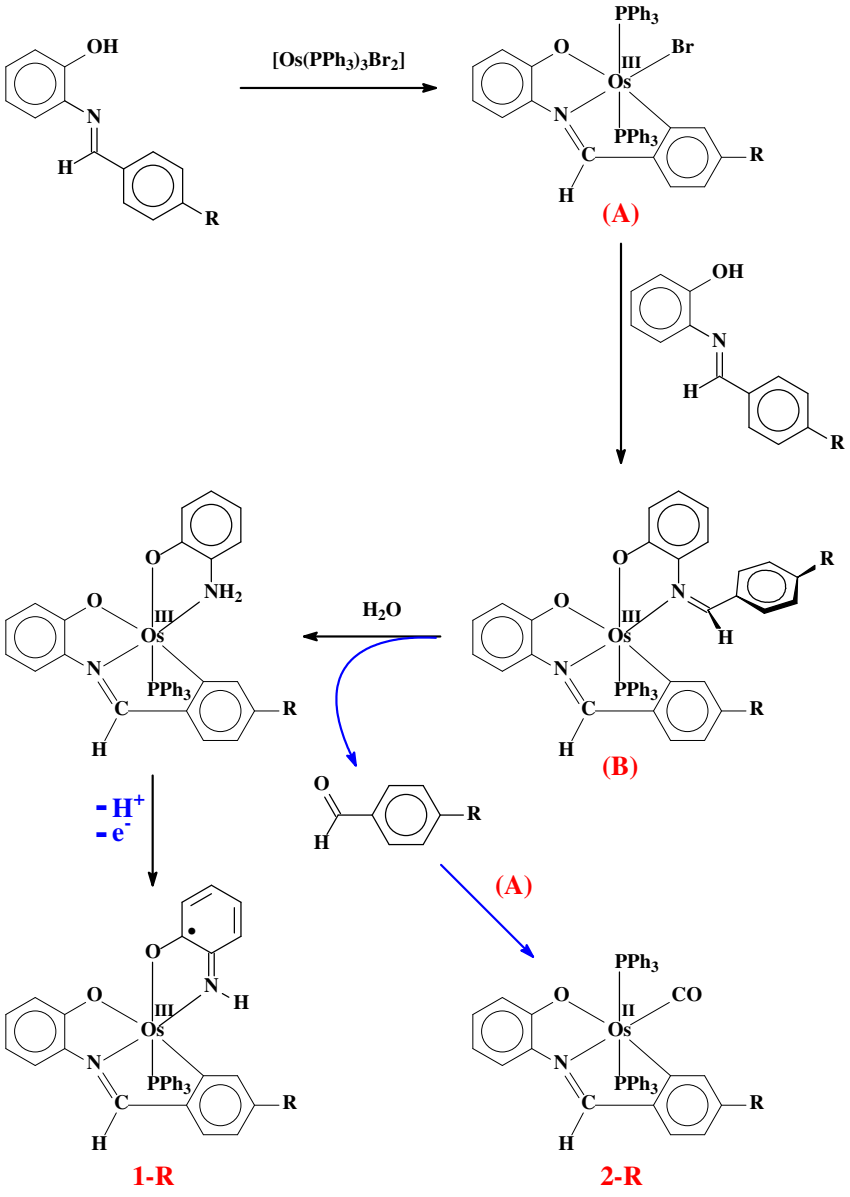

Scheme 1. Probable steps in the formation of complexes **1-R** and **2-R**.

these reactions did also afford the same **2-R** complexes. Hence it becomes apparent that the benzaldehyde, generated *in situ*, did serve as the source of carbonyl. Similar osmium mediated decarbonylation of aldehydes has been observed earlier [92].

2.2. Spectral studies

Magnetic susceptibility measurements show that both the **1-R** and **2-R** complexes are diamagnetic. From the composition of the **1-R** complexes, it is clear that osmium is in the +3 state (low-spin d^5, $S = 1/2$) in these complexes. The observed diamagnetism of these **1-R** complexes thus indicates that strong antiferromagnetic interaction between the unpaired electron on osmium and that on the iminosemiquinonate radical. It is relevant to mention in this context that similar antiferromagnetic interaction between an osmium(III) center and an iminosemiquinonate radical has been observed before [54]. The diamagnetic nature of the **2-R** complexes corresponds to the +2 oxidation state of osmium (low-spin d^6, $S = 0$) in them. ^{1}H NMR spectra of the **1-R** and **2-R** complexes have been recorded in $CDCl_3$ solution. Each complex shows broad signals within 7.1–7.5 ppm for the coordinated PPh_3 ligands. The azomethine proton signal is observed near 7.60 ppm and 7.08 ppm in the **1-R** and **2-R** complexes respectively. A distinct singlet is observed in the 6.38–6.84 ppm region in the **1-R** complexes with R = OCH_3, CH_3 and Cl and a similar signal is observed in the 4.71–5.95 ppm region in the corresponding **2-R** complexes with R ≠ H, which is assigned to the phenyl proton in between the metallated carbon and the substituent R (**II**, R ≠ H). Appearance of this signal confirms that orthometallation of the phenyl ring in the benzaldimine fragment has indeed taken place. In the **1-NO$_2$** complex this signal could not be identified, probably because of its overlap with other signals. Among the other expected aromatic proton signals for the C,N,O-coordinated ligand, most have been clearly observed while a few could not be detected due to their overlap with the PPh_3 signals. A distinct singlet is observed in all the **1-R** complexes at around 14.5 ppm, which is assigned to the N–H proton of the iminosemiquinonate fragment. Among the other expected aromatic proton signals for the C,N,O-coordinated ligand (and also

from the iminosemiquinonate ligand in the **1-R** complexes), most have been clearly observed while a few could not be detected due to their overlap with the PPh_3 signals. Infrared spectrum each **1-R** complex shows three strong bands near 518, 694 and 742 cm^{-1} indicating the presence of coordinated PPh_3 ligands [56,93–95]. A sharp band near 3270 cm^{-1} is also displayed by these complexes, which is attributable to the N–H stretch arising from the coordinated iminosemiquinonate fragment. Besides showing a strong band near 1895 cm^{-1} due to the coordinated carbon monoxide [96], infrared spectra of the **2-R** complexes are qualitatively similar to their respective **1-R** analogues. The ^1H NMR and IR spectral data of the **1-R** and **2-R** complexes are therefore consistent with their compositions.

The **1-R** and **2-R** complexes are soluble in acetone, dichloromethane, chloroform, etc., producing brown and bright blue solutions respectively. Electronic spectra of the complexes have been recorded in dichloromethane solution. Spectral data are presented in Table 2. All the complexes show several intense absorptions in the visible and ultraviolet regions. The absorptions in the ultraviolet region are attributable to transitions within the ligand orbitals and those in the visible region are probably due to charge-transfer transitions. Multiple charge-transfer transitions in such mixed-ligand complexes may result from the lower symmetry splitting of the metal level, the presence of different acceptor orbitals and from the mixing of singlet and triplet configurations in the excited state through spin-orbit coupling [97–100]. To have a better insight into the nature of the absorptions in the visible region, qualitative EHMO calculations have been performed [101,102] on computer generated models of the **1-R** and **2-R** complexes. Partial MO diagrams for two representative complexes are shown in Fig. 5 and Fig. S1 (Supplementary material), and compositions of selected molecular orbitals are given in Table S1 (Supplementary material). In the **1-R** complexes the highest occupied molecular orbital (HOMO) and the next two filled orbitals (HOMO-1 and HOMO-2) have

Table 2
Electronic spectral and cyclic voltammetric data.

Complex	Electronic spectral data[a] λ_{max}, nm (ε, M^{-1} cm^{-1})	Cyclic voltammetric data[b] E, V vs SCE
1-OCH_3	231(41 200), 312[c](18 600), 395(9700), 526(6600), 880(210)	0.47(80),[d] 1.16,[e] −1.02[f]
1-CH_3	231(26 100), 297[c](12 100), 400(7000), 518(4400), 859(150)	0.49(80),[d] 1.10,[e] −1.12[f]
1-H	231(20 900), 287[c](10 730), 400(5000), 515(3400), 859(190)	0.51(80),[d] 1.12,[e] −1.08[f]
1-Cl	231(39 200), 300[c](17 600), 400(8400), 518(5800), 859(140)	0.58(70),[d] 1.29,[e] −1.14[f]
1-NO_2	230(22 800), 296[c](10 100), 400(5500), 516(3600)	0.67(80),[d] 1.36,[e] −1.09[f]
2-OCH_3	235(34 600), 268[c](16 100), 312(13 500), 381(4600), 586(2500)	0.29(73),[d] 1.04(114),[d] −1.23[f]
2-CH_3	236(37 000), 272[c](13 300), 315(7000), 396(2400), 607(1200)	0.31(80),[d] 1.11(107),[d] −1.26[f]
2-H	234(37 700), 275[c](17 000), 314(13 500), 396(5900), 606(2400)	0.36(80),[d] 1.17(92),[d] −1.30[f]
2-Cl	234(39 300), 271[c](13 900), 315(6900), 395(2300), 607(1200)	0.41(80),[d] 1.29(83),[d] −1.31[f]
2-NO_2	240(51 600), 272[c](15 800), 349(1500), 438(800), 699(400)	0.51(70),[d] 1.11(79),[d] −1.16[f]

[a] In dichloromethane solution.
[b] Solvent, 1:9 dichloromethane–acetonitrile; supporting electrolyte, TBAP; reference electrode, SCE; $E_{1/2} = 0.5\ (E_{pa} + E_{pc})$, where E_{pa} and E_{pc} are anodic and cathodic peak potentials; $\Delta E_p = E_{pa} - E_{pc}$; scan rate, 50 mVs^{-1}.
[c] Shoulder.
[d] $E_{1/2}$ (ΔE_p, mV).
[e] E_{pa} value.
[f] E_{pc} value.

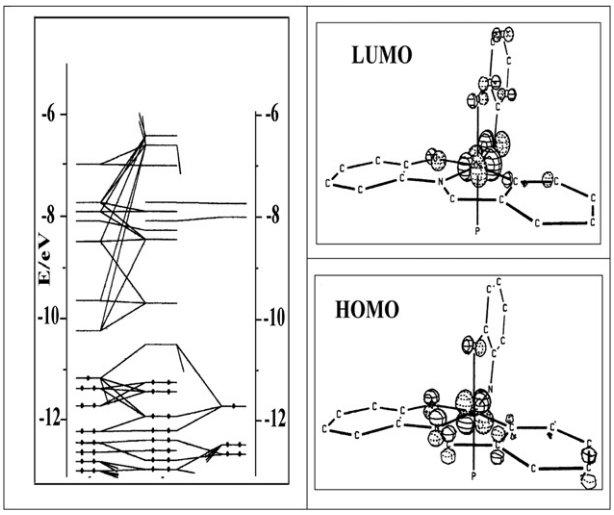

Fig. 5. Partial molecular orbital diagram of **1-H** complex.

major contributions from the osmium d_{xy}, d_{yz} and d_{zx} orbitals. These three occupied orbitals may therefore be regarded as the osmium t_2 orbitals. The lowest unoccupied molecular orbital (LUMO) has more than 60% contribution from the osmium ***e*** orbitals. Among the next few vacant orbitals, LUMO + 1 is primarily centered on the benzaldimine ligand and is concentrated mainly on the imine (C=N) fragment, while LUMO + 2 is delocalized over the C,N,O-coordinated benzaldimine ligand. The lowest energy absorption in the 850–880 nm region (Table 2), which is much less intense, may therefore be assigned to a d–d transition taking place from the highest filled osmium orbital (HOMO) to the lowest vacant orbital of the same (LUMO) [103]. The other intense absorptions at higher energies may be assigned to charge-transfer transitions from the osmium t_2 orbitals to the higher energy vacant orbitals. In the **2-R** complexes, the HOMO, HOMO-1 and HOMO-2 also have major contributions from the osmium d_{xy}, d_{yz} and d_{zx} orbitals. The LUMO, which is rather isolated, has more than 80% contribution from the benzaldimine ligand and is concentrated mainly on the imine (C=N) fragment. The LUMO + 1 is primarily centered on the carbonyl ligand, while LUMO + 2 is delocalized over both the phenyl rings of the benzaldimine ligand. The intense and rather isolated absorption in the 586–699 nm region may therefore be assigned to the charge-transfer transition taking place from the highest filled osmium t_2 orbital (HOMO) to the vacant π^*(C=N) orbital of the benzaldimines (LUMO). The other intense absorptions at higher energies may be assigned to charge-transfer transitions from the osmium t_2 orbitals to the higher energy vacant orbitals.

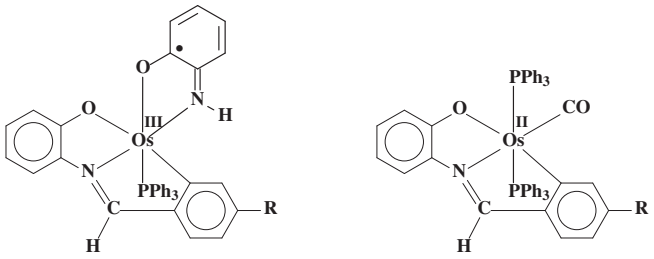

1-R **2-R**

Chart 1.

2.3. Electrochemical properties

Electrochemical properties of the **1**-**R** and **2**-**R** complexes have been studied by cyclic voltammetry in 1:9 dichloromethane-acetonitrile solution (0.1 M TBAP) [104]. Voltammetric data are given in Table 2. Each **1**-**R** complex shows an oxidative response within 0.47–0.67 V vs SCE, and in view of composition of the HOMO in these complexes this oxidation is assigned to the Os(III)–Os(IV) oxidation. This oxidation is reversible, characterized by a peak-to-peak separation (ΔE_p) of 70–80 mV, which remains unchanged upon changing the scan rate, and the anodic peak current (i_{pa}) is almost equal to the cathodic peak current (i_{pc}), as expected for a reversible electron-transfer process. The **1**-**R** complexes show a second oxidative response within 1.10–1.36 V vs SCE, which is tentatively assigned to the oxidation of the iminosemiquinonate ligand. One-electron nature of both the oxidations has been verified by comparing their current heights (i_{pa}) with that of the standard ferrocene/ferrocenium couple under identical experimental conditions. Potential of the Os(III)–Os(IV) oxidation has been found to be sensitive to the nature of the substituent R in the C,N,O-coordinated benzaldimine ligand. The potential ($E_{1/2}$) increases with increasing electron-withdrawing character of the substituent R. The plot of $E_{1/2}$ vs σ [σ = Hammett constant of R [105]; $OCH_3 = -0.27$, $CH_3 = -0.17$, H = 0.00, Cl = 0.23 and $NO_2 = 0.78$] is linear (Figure S2, Supplementary material) with a slope (ρ) of 0.19 V (ρ = reaction constant of this couple) [106]. This linear correlation of $E_{1/2}$ vs σ with a reasonable slope (ρ) clearly shows that a single substituent on the C,N,O-coordinated benzaldimine can influence the metal-centered oxidation potential in a predictable manner. The **1**-**R** complexes show an irreversible reduction within −1.02 to −1.14 V vs SCE, which is assigned, in view of composition of the LUMO, to Os(III)–Os(II) reduction. Potential of this irreversible reduction does not show any systematic variation with the nature of the substituent R. The **2**-**R** complexes show two oxidative responses on the positive side of SCE. The first response, observed within 0.29–0.51 V, is reversible in nature and is assigned to the Os(II)–Os(III) oxidation based on the HOMO composition. The second oxidative response, observed within 1.04–1.29 V, is quasi-reversible in nature and is tentatively assigned to Os(III)–Os(IV) oxidation. Potential of the Os(II)–Os(III) oxidation correlates linearly with the electron-withdrawing character (σ) of the substituent R, with a slope (ρ) of 0.21 V (Figure S3, supporting material), however, that of the second oxidation does not show similar correlation. The **2**-**R** complexes also show an irreversible reduction within −1.16 to −1.31 V vs SCE, which is assigned, in view of the LUMO composition, to reduction of the coordinated benzaldimine, and potential of this reduction does not show any linear correlation with the nature of the substituent R.

3. Conclusions

The present study shows that the N-(2′-hydroxyphenyl)-4-R-benzaldimines (**L**-**R**) can undergo C–H activation, as well as hydrolytic cleavage of the imine bond, upon reaction with $[Os(PPh_3)_3Br_2]$. This study also demonstrates that benzaldehydes can undergo facile osmium-assisted decarbonylation, yielding carbonyl complexes. The present study thus indicates that C–H activation of selective organic substrates, having skeletal similarity with the benzaldimines (**L**–**R**), may be achievable by their reaction with $[Os(PPh_3)_3Br_2]$ leading to the formation of interesting organoosmium complexes.

4. Experimental

Microanalyses (C, H, N) were performed using a Heraeus Carlo Erba 1108 elemental analyzer. Magnetic susceptibilities were measured using a PAR 155 Vibrating sample magnetometer fitted with a Walker scientific L75FBAL magnet. ^{1}H NMR spectra were recorded in $CDCl_3$ solution on a Bruker Avance DPX 300 NMR spectrometer using TMS as the internal standard. IR spectra were obtained on a Shimadzu FTIR-8300 spectrometer with samples prepared as KBr pellets. Electronic spectra were recorded on a JASCO V-570 spectrophotometer. Electrochemical measurements were made using a CH Instruments model 600A electrochemical analyzer. A platinum disc working electrode, a platinum wire auxiliary electrode and an aqueous saturated calomel reference electrode (SCE) were used in the cyclic voltammetry experiments. All electrochemical experiments were performed under a dinitrogen atmosphere. All electrochemical data were collected at 298 K and are uncorrected for junction potentials. Commercial osmium tetroxide was purchased from Arora Matthey, Kolkata, India and was converted to $[NH_4]_2[OsBr_6]$ by reduction with hydrobromic acid [107]. Triphenylphosphine, 2-aminophenol and the *para*-substituted benzaldehydes were obtained from Merck, India. $[Os(PPh_3)_3Br_2]$ was synthesized, starting from $[NH_4]_2[OsBr_6]$, by following a reported procedure [108]. The N-(2′-hydroxyphenyl) benzaldimines (**L**-**R**) were prepared by reacting equimolar amounts of respective *para*-substituted benzaldehyde and 2-aminophenol in ethanol. Purification of acetonitrile and preparation of tetrabutylammonium perchlorate (TBAP) for electrochemical work were performed as reported in the literature [109,110]. All other chemicals and solvents were reagent grade commercial materials and were used as received.

4.1. Synthesis of complexes

The **1**-**R** and **2**-**R** complexes were synthesized by following a general procedure. Specific details are given below for one pair of complexes.

1-$\mathbf{OCH_3}$ and **2**-$\mathbf{OCH_3}$. N-(2′-hydroxyphenyl)-4-methoxybenzaldimine (20 mg, 0.09 mmol) was dissolved in 2-methoxyethanol (50 mL) and triethylamine (18 mg, 0.18 mmol) was added to it and was warmed. To the warm solution was added $[Os(PPh_3)_3Br_2]$ (100 mg, 0.09 mmol) and the mixture was refluxed for 24 h, whereby a brown solution was obtained. Evaporation of this solution afforded a dark solid, which was subjected to purification by thin layer chromatography on a silica plate. With 1:10 acetonitrile–benzene as the eluant, a distinct blue band separated first followed by a brown band, both of which were extracted with 1:3 dichoromethane–acetonitrile. Evaporation of the brown extract gave **1**-$\mathbf{OCH_3}$ as a crystalline brown solid and that of the blue extract gave **2**-$\mathbf{OCH_3}$ as a crystalline blue solid.

1-$\mathbf{OCH_3}$**:** Yield: 21%. Anal. Calc. for $C_{38}H_{31}O_3N_2POs$: C, 58.16; H, 3.95; N, 3.57. Found: C, 58.18; H, 3.87; N, 3.55%. ^{1}H NMR [111]: 3.38 (OCH_3); 4.71(s, H); 5.75 (d, H, J = 8.2); 6.22 (t, H, J = 7.5); 6.35 (d, H, J = 8.2); 6.68 (t, H, J = 7.5); 6.81 (t, H, J = 9.4); 6.93–6.96* (2H); 7.09 (d, H, J = 8.3); 7.26–7.38 (PPh_3); 7.47–7.49* (2H); 14.64 (s, H). **1**-$\mathbf{CH_3}$**:** Yield: 22%. Anal. Calc. for $C_{38}H_{31}O_2N_2POs$: C, 59.37; H, 4.03; N, 3.64. Found: C, 59.35; H, 3.95; N, 3.62%. ^{1}H NMR: 2.34 (CH_3); 4.84 (s, H); 6.00 (d, H, J = 7.6); 6.24 (t, H, J = 7.5); 6.38 (d, H, J = 8.2); 6.68 (t, H, J = 6.2); 6.83 (t, H, J = 7.5); 6.97–7.0* (2H); 7.15 (d, H, J = 7.0); 7.26–7.41 (PPh_3); 7.49 (d, H, J = 8.4); 7.58 (s, H); 14.2 (s, H). **1**-**H:** Yield: 20%. Anal. Calc. for $C_{37}H_{29}O_2N_2POs$: C, 58.88; H, 3.84; N, 3.71. Found: C, 58.80; H, 3.79; N, 3.68%. ^{1}H NMR: 4.81 (s, H); 5.08 (d, H, J = 7.6); 6.15–6.25* (2H); 6.34–6.42* (2H); 6.59 (t, H, J = 8.0); 6.69 (t, H, J = 7.4); 6.97 (d, H, J = 8.1); 6.99 (d, 1H, J = 4.6); 7.10 (d, 2H, J = 7.9); 7.26–7.38 (PPh_3); 7.46–7.50* (2H); 14.58 (s, H). **1**-**Cl:** Yield: 20%. Anal. Calc. for $C_{37}H_{28}O_2N_2ClPOs$: C, 56.30; H, 3.55; N, 3.55. Found: C, 56.75; H, 3.47; N, 3.50%. ^{1}H NMR: 5.03 (s, H); 6.20 (d, H, J = 8.3); 6.28 (t, H, J = 7.5); 6.39 (d, H, J = 8.2); 6.71 (t, H, J = 7.4); 6.86 (t, H, J = 7.4); 6.93 (d, H, J = 8.1); 6.99 (d, H, J = 8.0); 7.16 (d, H,

$J = 8.1$); 7.31–7.37 (PPh_3); 7.50 (d, H, $J = 8.5$); 7.60 (s, H); 14.2 (s, H). **1-NO_2:** Yield: 20%. Anal. Calc. for $C_{37}H_{28}O_4N_3POs$: C, 55.50; H, 3.50; N, 5.25. Found: C, 55.48; H, 3.44; N, 5.21%. ^{1}H NMR: 5.95 (s, H); 6.27 (t, H, $J = 7.5$); 6.39 (d, H, $J = 8.3$); 6.74 (d, H, $J = 7.4$); 6.88 (t, H, $J = 7.7$); 7.08* (2H); 7.17–7.20* (2H); 7.26–7.39 (PPh_3); 7.48 (d, H, $J = 8.2$); 7.67 (s, H); 14.15 (s, H).

2-OCH_3: Yield: 20%. Anal. Calc. for $C_{51}H_{41}O_3NP_2Os$: C, 63.29; H, 4.23; N, 1.45. Found: C, 63.24; H, 4.35; N, 1.43%. ^{1}H NMR: 3.53 (OCH_3); 5.66 (t, H, $J = 7.5$); 5.76(d, H, $J = 7.2$); 5.98 (d, H, $J = 8.7$); 6.36–6.40* (2H); 6.60 (d, H, $J = 8.4$); 7.06 (s, H); 7.16 (s, H); 7.16–7.46 (2PPh_3). **2-CH_3:** Yield: 21%. Anal. Calc. for $C_{51}H_{41}O_2NP_2Os$: C, 64.35; H, 4.31; N, 1.47. Found: C, 64.73; H, 4.29; N, 1.45%. ^{1}H NMR: 2.45 (CH_3); 5.65 (t, H, $J = 7.3$); 5.76(d, H, $J = 7.6$); 5.99 (d, H, $J = 8.2$); 6.18 (d, H, $J = 7.5$); 6.39 (t, H, $J = 7.5$); 6.56 (d, H, $J = 7.6$); 6.70 (s, H); 7.08 (s, H); 7.19–7.45 (2PPh_3). **2-H:** Yield: 20%. Anal. Calc. for $C_{50}H_{39}O_2NP_2Os$: C, 64.03; H, 4.16; N, 1.49. Found: C, 64.56; H, 4.20; N, 1.49%. ^{1}H NMR: 5.65 (t, H, $J = 7.4$); 5.77 (d, H, $J = 7.6$); 5.93 (d, H, $J = 8.3$); 6.28–6.41* (3H); 6.61 (d, H, $J = 7.0$); 7.00–7.04* (2H); 7.13 (s, H); 7.19–7.55 (2PPh_3). **2-Cl:** Yield: 20%. Anal. Calc. for $C_{50}H_{38}O_2NClP_2Os$: C, 61.76; H, 3.91; N, 1.44. Found: C, 61.65; H, 3.80; N, 1.46%. ^{1}H NMR: 5.67 (t, H, $J = 7.2$); 5.77 (d, H, $J = 7.6$); 5.97 (d, H, $J = 8.3$); 6.35(d, H, $J = 8.2$); 6.40 (t, H, $J = 7.3$); 6.52 (d, H, $J = 8.0$); 6.84 (s, H); 7.08 (s, H); 7.19–7.44 (2PPh_3). **2-NO_2:** Yield: 20%. Anal. Calc. for $C_{50}H_{38}O_4N_2P_2Os$: C, 61.09; H, 3.86; N, 2.85. Found: C, 61.62; H, 3.74; N, 2.93%. ^{1}H NMR: 5.66 (t, H, $J = 7.4$); 5.75(d, H, $J = 7.8$); 5.97 (d, H, $J = 8.4$); 6.40 (t, H, $J = 6.9$); 6.59(d, H, $J = 8.4$); 7.03–7.13* (2H); 7.19–7.41 (2PPh_3).

4.2. X-ray crystallography

Single crystals of the **1-Cl** and **2-OCH_3** complexes were obtained by slow diffusion of hexane into a dichloromethane solution of the respective complexes. All data were collected at 120 K. Selected crystal data and data collection parameters are given in Table 3. Data were collected on a Bruker APEX diffractometer fitted with a Bede Microsource using graphite monochromated MoKα radiation ($\lambda = 0.71073$ Å) by 2θ–ω scans within the θ range of 3.6–28.50° and 3.5 to 28.30° respectively. X-ray data reduction, structure solution and refinement were done using standard Bruker software programs [112]. The structures were solved by the direct methods. All data were corrected for absorption with SADABS [113]. Refinement was on F^2 using full–matrix least-squares technique. All hydrogen atoms were placed at calculated position and refined using a riding model, with the exception of the water hydrogen atoms which were located in the fourier difference map and fixed at 0.86 Å from O7.

Table 3
Crystallographic data for **1-Cl** and **2-OCH_3**.

	1-Cl	2-OCH_3·0.375H_2O
Empirical formula	$C_{37}H_{28}ClN_2O_2OsP$	$C_{51}H_{41}O_3NP_2Os.0.375H_2O$
Formula weight	789.23	974.74
Space group	Triclinic, P1	Monoclinic, $P2_1$
a (Å)	9.7552(10)	11.9981(6)
b (Å)	13.0640(13)	17.5010(8)
c (Å)	14.1147(14)	20.0110(9)
α (deg)	102.132(4)	90
β (deg)	107.410(6)	90.085(1)
γ (deg)	108.635(6)	90
V(Å^3)	1530.6(3)	4203.0(16)
Z	2	4
λ (Å)	0.71073	0.71073
Crystal size (mm)	0.08 × 0.11 × 0.16	0.17 × 0.25 × 0.40
T (K)	120	120
μ (mm^{-1})	4.343	3.157
R_1[a]	0.0237	0.0219
wR_2[b]	0.0550	0.0469
Goodness-of-fit (GOF)[c]	1.05	0.95

[a] $R_1 = \Sigma\acute{u}\acute{u}F_o\acute{u} - \acute{u}\,F_c\acute{u}\acute{u}/\Sigma\acute{u}\,F_o\acute{u}$.
[b] $wR_2 = [\Sigma\{w(F_o^2 - F_c^2)^2\}/\Sigma\{w(F_o^2)\}]^{1/2}$.
[c] GOF = $[\Sigma(w(F_o^2 - F_c^2)^2)/(M - N)]^{1/2}$, where M is the number of reflections and N is the number of parameters refined.

Acknowledgements

The authors thank the reviewers for their constructive comments, which have been helpful in preparing the revised manuscript. Financial assistance received from the UGC CAS Program of the Department of Chemistry, Jadavpur University, is gratefully acknowledged. The authors thank Ms Sayanti Dutta for her help in preparing the manuscript. JAKH and HAS are grateful to the EPSRC for funding.

Appendix A. Supplementary material

CCDC-764096 and -764097 contain the supplementary crystallographic data for this paper. These data can be obtained free of charge from The Cambridge Crystallographic Data Centre via www.ccdc.cam.ac.uk/data_request/cif.

Partial molecular orbital diagram of the **2-H** complex (Fig. S1), least-squares plot of $E_{1/2}$ values of Os(III)–Os(IV) couple vs σ for the **1-R** complexes (Fig. S2), least-squares plot of $E_{1/2}$ values of Os (II)–Os(III) couple σ for the **2-R** complexes (Fig. S3), and composition of selected molecular orbitals for the **1-R** and **2-R** complexes (Table S1).

Supplementary data associated with this article can be found, in the online version, at doi:10.1016/j.jorganchem.2010.05.015.

References

[1] N.A. Foley, J.P. Lee, Z. Ke, T.B. Gunnoe, T.R. Cundari, Acc. Chem. Res. 42 (2009) 585.
[2] B.H. Lipshutz, Y. Yamamoto, Chem. Rev. 108 (2008) 2793.
[3] T. Mallat, A. Baiker, Chem. Rev. 104 (2004) 3037.
[4] B.M. Trost, M.L. Crawley, Chem. Rev. 103 (2003) 2921.
[5] C.M. Che, J.S. Huang, Coord. Chem. Rev. 242 (2003) 97.
[6] F. Alonso, I.P. Beletskaya, M. Yus, Chem. Rev. 102 (2002) 4009.
[7] A. de Meijere, Chem. Rev. 100 (2000) 2739.
[8] J. Tsuji, Transition Metal Reagents and Catalysts. Wiley-VCH, Weinheim, 2000.
[9] L.S. Hegedus, Coord. Chem. Rev. 168 (1998) 49.
[10] M. Bellar, C. Bolm (Eds.), Transition Metals for Organic Synthesis, vol. 1–2, Wiley-VCH, Weinheim, 1998.
[11] B. Cornils, W.A. Hermann (Eds.), Applied Homogenous Catalysis with Organometallic Compounds: a Comprehensive Handbook in Two Volumes, VCH, Weinheim, 1996.
[12] L.S. Liebeskind (Ed.), Advances in Metal-Organic Chemistry, Jai Press, Greenwich, CT, 1996.
[13] E. Abel, F.G.A. Stone, G. Wilkinson (Eds.), Comprehensive Organometallic Chemistry, Pergamon Press, Oxford, 1995, p. 12.
[14] L.S. Hegedus, Transition Metals in the Synthesis of Complex Organic Molecules. Mill Valley, CA, 1994.
[15] J.P. Collman, L.S. Hegedus, J.R. Norton, R.G. Finke, Principles and Applications of Organotransition Metal Chemistry. Mill Valley, CA, 1987.
[16] B.M. Trost, T.R. Verhoeven, in: E. Abel, F.G.A. Stone, G. Wilkinson (Eds.), Comprehensive Organometallic Chemistry, Pergamon Press, Oxford, 1982, p. 8.
[17] O. Daugulis, H.Q. Do, D. Shabashov, Acc. Chem. Res. 42 (2009) 1074.
[18] J.C. Lewis, R.G. Bergman, J.A. Ellman, Acc. Chem. Res. 41 (2008) 1013.
[19] Y.J. Park, J.W. Park, C.H. Jun, Acc. Chem. Res. 41 (2008) 222.
[20] W. Leis, H.A. Mayer, W.C. Kaska, Coord. Chem. Rev. 252 (2008) 1787.
[21] M. Lersch, M. Tilset, Chem. Rev. 105 (2005) 2471.
[22] E. Carmona, M. Paneque, L.L. Santos, V. Salazar, Coord. Chem. Rev. 249 (2005) 1729.
[23] H.A.Y. Mohammad, J.C. Grimm, K. Eichele, H.G. Mack, B. Speiser, F. Novak, W. C. Kaska, H.A. Mayer, Activation and Functionalization of C–H Bonds (2004) pp. 234–247 (Chapter 14).
[24] P. Legzdins, C.B. Pamplin, Activation and Functionalization of C–H Bonds (2004) pp. 184–197 (Chapter 11).
[25] S.R. Klei, K.L. Tan, J.T. Golden, C.M. Yung, R.K. Thalji, K.A. Ahrendt, J.A. Ellman, T.D. Tilley, R.G. Bergman, Activation and Functionalization of C–H Bonds (2004) pp. 46–55 (Chapter 2).
[26] H.-Y. Jang, M.J. Krische, Acc. Chem. Res. 37 (2004) 653.
[27] M.E.V. Boom, D. Milstein, Chem. Rev. 103 (2003) 1759.
[28] C.B. Pamplin, P. Legzdins, Acc. Chem. Res. 36 (2003) 223.
[29] K. Matsumoto, H. Sugiyama, Acc. Chem. Res. 35 (2002) 915.

[30] C.S. Chin, G. Won, D. Chong, M. Kim, H. Lee, Acc. Chem. Res. 35 (2002) 218.
[31] V. Ritleng, C. Sirlin, M. Pfeffer, Chem. Rev. 102 (2002) 1731.
[32] K. Matsumoto, M. Ochiai, Coord. Chem. Rev. 231 (2002) 229.
[33] A. Vigalok, D. Milstein, Acc. Chem. Res. 34 (2001) 798.
[34] C. Slugovc, I. Padilla-Martnez, S. Sirol, E. Carmona, Coord. Chem. Rev. 213 (2001) 129.
[35] C. Jia, T. Kitamura, Y. Fujiwara, Acc. Chem. Res. 34 (2001) 633.
[36] R. Acharyya, S.M. Peng, G.H. Lee, S. Bhattacharya, J. Chem. Sci. 121 (2009) 387.
[37] S. Dutta, F. Basuli, A. Castineiras, S.M. Peng, G.H. Lee, S. Bhattacharya, Eur. J. Inorg. Chem. (2008) 4538.
[38] M. Dasgupta, H. Tadesse, A.J. Blake, S. Bhattacharya, J. Organomet. Chem. 693 (2008) 3281.
[39] S. Baksi, R. Acharyya, F. Basuli, S.M. Peng, G.H. Lee, M. Nethaji, S. Bhattacharya, Organometallics 26 (2007) 6596.
[40] C. GuhaRoy, S.S. Sen, S. Dutta, G. Mostafa, S. Bhattacharya, Polyhedron 26 (2007) 3876.
[41] S. Nag, R.J. Butcher, S. Bhattacharya, Eur. J. Inorg. Chem. (2007) 1251.
[42] S. Baksi, R. Acharyya, S. Dutta, A.J. Blake, M.G.B. Drew, S. Bhattacharya, J. Organomet. Chem. 692 (2007) 1025.
[43] S. Halder, M.G.B. Drew, S. Bhattacharya, Organometallics 25 (2006) 5969.
[44] S. Halder, R. Acharyya, S.M. Peng, G.H. Lee, M.G.B. Drew, S. Bhattacharya, Inorg. Chem. 45 (2006) 9654.
[45] S. Basu, S. Dutta, M.G.B. Drew, S. Bhattacharya, J. Organomet. Chem. 691 (2006) 3581.
[46] R. Acharyya, S. Dutta, F. Basuli, S.M. Peng, G.H. Lee, L.R. Falvello, S. Bhattacharya, Inorg. Chem. 45 (2006) 1252.
[47] P. Gupta, S. Dutta, F. Basuli, S.M. Peng, G.H. Lee, S. Bhattacharya, Inorg. Chem. 45 (2006) 460.
[48] R. Acharyya, F. Basuli, S.M. Peng, G.H. Lee, R.Z. Wang, T.C.W. Mak, S. Bhattacharya, J. Organomet. Chem. 690 (2005) 3908.
[49] S. Nag, P. Gupta, R.J. Butcher, S. Bhattacharya, Inorg. Chem. 43 (2004) 4814.
[50] R. Acharyya, F. Basuli, R.Z. Wang, T.C.W. Mak, S. Bhattacharya, Inorg. Chem. 43 (2004) 704.
[51] R. Acharyya, S.M. Peng, G.H. Lee, S. Bhattacharya, Inorg. Chem. 42 (2003) 7378.
[52] P. Gupta, R.J. Butcher, S. Bhattacharya, Inorg. Chem. 42 (2003) 5405.
[53] I. Pal, S. Dutta, F. Basuli, S. Goverdhan, S.M. Peng, G.H. Lee, S. Bhattacharya, Inorg. Chem. 42 (2003) 4338.
[54] K. Majumder, S.M. Peng, S. Bhattacharya, J. Chem. Soc. Dalton Trans. (2001) 284.
[55] A. Das, F. Basuli, L.R. Falvello, S. Bhattacharya, Inorg. Chem. 40 (2001) 4085.
[56] F. Basuli, S.M. Peng, S. Bhattacharya, Inorg. Chem. 40 (2001) 1126.
[57] S. Dutta, S.M. Peng, S. Bhattacharya, J. Chem. Soc. Dalton Trans. (2000) 4623.
[58] A. Albinati, C. Arz, P.S. Pregosin, J. Organomet. Chem. 335 (1987) 379.
[59] P. Ghosh, A. Pramanik, N. Bag, G.K. Lahiri, A. Chakravorty, J. Organomet. Chem. 454 (1993) 237.
[60] C. Lopez, A. Caubet, S. Perez, X. Solans, M.F. Bardia, J. Organomet. Chem. 68 (2003) 82.
[61] C.L. Gross, G.S. Girolami, Organometallics 25 (2006) 4792.
[62] R.M. Gauvin, H. Rozenberg, L.J.W. Shimon, D. Milstein, Organometallics 20 (2001) 1719.
[63] H. Werner, T. Daniel, O. Nürnberg, W. Knaup, U. Meyer, J. Organomet. Chem. 445 (1993) 229.
[64] P.K. Nanda, D. Mandal, D. Ray, Polyhedron 25 (2006) 702.
[65] P. Marcazzan, B.O. Patrick, B.R. James, Organometallics 24 (2005) 1445.
[66] P. Marcazzan, C. Abu-Gnim, K.N. Seneviratne, B.R. James, Inorg. Chem. 43 (2004) 4820.
[67] C.E.F. Rickard, W.R. Roper, A. Williamson, L.J. Wright, Organometallics 21 (2002) 4862.
[68] C.E.F. Rickard, W.R. Roper, A. Williamson, L.J. Wright, Organometallics 21 (2002) 1714.
[69] C.E.F. Rickard, W.R. Roper, S.D. Woodgate, L.J. Wright, J. Organomet. Chem. 643 (2002) 169.
[70] K. Pramanik, M. Shivakumar, P. Ghosh, A. Chakravorty, Inorg. Chem. 39 (2000) 195.
[71] A. Das, F. Basuli, S.M. Peng, S. Bhattacharya, Polyhedron 18 (1999) 2729.
[72] P.D. Robinson, C.C. Hinckley, A. Ikuo, Acta Cryst. C44 (1988) 1491.
[73] G. Bellachioma, G. Cardaci, A. Macchioni, P. Zanazzi, Inorg. Chem. 32 (1993) 547.
[74] S.K. Burley, G.A. Petsko, Science 229 (1985) 23.
[75] H.C. Weiss, D. Blaser, R. Boese, B.M. Doughan, M.M. Haley, Chem. Commun. (1997) 1703.
[76] N.N.L. Madhavi, A.K. Katz, H.L. Carrell, A. Nangia, G.R. Desiraju, Chem. Commun. (1997) 1953.
[77] S.K. Burley, G.A. Petsko, Adv. Protein Chem. 39 (1988) 125.
[78] M. Nishio, M. Hirota, Y. Umezawa, The CH···π interactions (Evidence, Nature and Consequences). Wiley-VCH, New York, 1998.
[79] Y. Umezawa, S. Tsuboyama, K. Honda, J. Uzawa, M. Nishio, Bull. Chem. Soc. Jpn. 71 (1998) 1207.
[80] G.R. Desiraju, T. Steiner, The Weak Hydrogen Bond (IUCr Monograph on Crystallography 9). Oxford Science Pub, 1999.
[81] M.J. Hannon, C.L. Painting, N.W. Alcock, Chem. Commun. (1999) 2023.
[82] B.J. Mcnelis, L.C. Nathan, C.J. Clark, J. Chem. Soc. Dalton Trans. (1999) 1831.
[83] K. Biradha, C. Seward, M.J. Zaworotko, Angew. Chem. Int. Ed. 38 (1999) 492.
[84] M.J. Calhorda, Chem. Commun. (2000) 801.
[85] C. Janiak, S. Temizdemir, S. Dechert, Inorg. Chem. Commun. 3 (2000) 271.
[86] C. Janiak, S. Temizdemir, S. Dechert, W. Deck, F. Girgsdies, J. Heinze, M. J. Kolm, T.G. Scarmann, O.M. Zipffel, Eur. J. Inorg. Chem. (2000) 1229.
[87] D.G. Gusev, F.M. Dolgushin, M.Y. Antipin, Organometallics 21 (2002) 1001.
[88] P. Barrio, M.A. Esteruelas, E. Õnate, Organometallics 21 (2002) 1714.
[89] F. Basuli, S.M. Peng, S. Bhattacharya, Polyhedron 18 (1998) 391.
[90] S. Bhattacharya, P. Gupta, F. Basuli, C.G. Pierpont, Inorg. Chem. 41 (2002) 5810.
[91] C.N. Verani, S. Gallert, E. Bill, T. Weyhermuller, K. Wieghardt, P. Chaudhuri, Chem. Commun. (1999) 410.
[92] P. Gupta, F. Basuli, S.M. Peng, G.H. Lee, S. Bhattacharya, Indian J. Chem. 42A (2003) 2406.
[93] S. Dutta, F. Basuli, S.M. Peng, G.H. Lee, S. Bhattacharya, New J. Chem. 26 (2002) 1607.
[94] A.K. Das, S.M. Peng, S. Bhattacharya, J. Chem. Soc. Dalton Trans. (2000) 181.
[95] S. Dutta, S.M. Peng, G.H. Lee, S. Bhattacharya, Inorg. Chem. 39 (2000) 2231.
[96] J.W. Diluzio, L. Vaska, J. Am. Chem. Soc. 83 (1961) 1262.
[97] B.J. Pankuch, D.E. Lacky, G.A. Crosby, J. Phys. Chem. 84 (1980) 2061.
[98] A. Ceulemans, L.G. Vanquickenborne, J. Am. Chem. Soc. 103 (1981) 2238.
[99] S. decuritus, F. Felix, J. Ferguson, H.U. Gudel, A. Ludi, J. Am. Chem. Soc. 103 (1980) 4102.
[100] E.M. Kober, T.J. Meyer, Inorg. Chem. 21 (1982) 3967.
[101] C. Mealli, D.M. Proserpio, CACAO Version 4.0 Italy (1994).
[102] C. Mealli, D.M. Proserpio, J. Chem. Educ. 67 (1990) 399.
[103] This d–d transition could not be observed for **1**-NO_2. In this complex the LUMO is primarily spread over the benzaldimine ligand and is concentrated heavily on the imine (C=N) fragment.
[104] A little dichloromethane was necessary to take the complex into solution. Addition of large excess of acetonitrile was necessary to record the redox responses in proper shape.
[105] L.P. Hammett, Physical Organic Chemistry, second ed. McGraw Hill, New York, 1970.
[106] R.N. Mukherjee, O.A. Rajan, A. Chakravorty, Inorg. Chem. 21 (1982) 785.
[107] F.P. Dwyer, J.W. Hogarth, Inorg. Synth. 5 (1957) 204.
[108] P.R. Hoffman, K.G. Caulton, J. Am. Chem. Soc. 97 (1975) 4221.
[109] D.T. Sawyer, J.L. Roberts Jr., Experimental Electrochemistry for Chemists. Wiley, New York, 1974, 167–215.
[110] M. Walter, L. Ramaley, Anal. Chem. 45 (1973) 165.
[111] Chemical shifts are given in ppm and multiplicity of the signals along with the associated coupling constants (J in Hz) are given in parentheses. Overlapping signals are marked with an asterisk.
[112] Bruker, SMART-NT Version 5.0 (Data Collection), SAINT Version 6.45A (Data Processing), and SHELXTL Version 6.1 (Structure Solution, and Refinement). Bruker AXS Inc., Madison, Wisconsin, USA, 2001.
[113] A.L. Spek, J. Appl. Cryst 36 (2003) 7.